J. Phys.: Condens. Matter **12** (2000) 2265–2278. Printed in the UK PII: S0953-8984(00)08916-5

Neutron powder diffraction study of the $RFe_{11.5}Ta_{0.5}$ (R ≡ Lu, Er, Ho, Dy and Tb) compounds

C Piquer†, E Palacios†, M Artigas†, J Bartolomé†, J Rubín†, J Campo‡ and M Hofmann§

† Instituto de Ciencia de Materiales de Aragón, Consejo Superior de Investigaciones Científicas, Universidad de Zaragoza, 50009, Zaragoza, Spain
‡ Institut Laue–Langevin, BP 156, 38042 Grenoble Cédex 9, France
§ Hahn-Meitner Institut, Berlin Neutron Scattering Centre, D-14109, Berlin, Germany

Received 20 October 1999

Abstract. We report a systematic study of the crystallographic and magnetic structures of the $RFe_{11.5}Ta_{0.5}$ (R ≡ Lu, Er, Ho, Dy and Tb) compounds carried out by means of neutron powder diffraction. Thermal dependencies of lattice parameters, magnetic moments and magnetization directions have been determined. The hierarchy of the Fe magnetic moments at the 8i, 8j and 8f sites was found to be $\mu_{8i} > \mu_{8j} \geqslant \mu_{8f}$ for all compounds at all temperatures. The influence of the atomic environments on the strength of the Fe local moments at each of the crystallographic sites is discussed. The results of the magnetic refinement are compared to those previously obtained from magnetic measurements on the same compounds.

1. Introduction

Rare-earth (R) iron-rich intermetallic compounds with $ThMn_{12}$ structure (with space group $I4/mmm$, $Z = 2$) are very interesting since they present relatively high Curie temperature T_c and saturation magnetization M_s, and a crystal structure simpler than that of the $R_2Fe_{14}B$ or R_2Fe_{17} compounds [1, 2]. The R atoms are located at just one crystallographic site, the Th (2a) site, while the Fe atoms are distributed over the 8i, 8j and 8f Mn sites.

Pure RFe_{12} is not stable. A non-magnetic third element M is needed to stabilize the $ThMn_{12}$ structure—forming the $RFe_{12-x}M_x$ pseudo-binary compounds. However, the presence of such non-magnetic elements has a detrimental influence on the magnetic properties of these compounds [1]. Consequently, one of the research avenues associated with the $RFe_{12-x}M_x$ compounds is the synthesis of new phases with the minimal amount of stabilizing agent. Recently we have reported on the synthesis of the new compounds $RFe_{11.5}Ta_{0.5}$, with R ≡ Tb, Dy, Ho, Er and Lu [3], in which the M substitution is minimum—just comparable to that of $YFe_{11.5}Mo_{0.5}$ [4].

In a previous work we studied the macroscopic magnetic properties of the title compounds: T_c, magnetic anisotropy at room temperature (RT) and spin-reorientation transitions, by means of ac susceptibility, magnetization versus temperature and field, and x-ray diffraction [3]. The main results are summarized in table 1. Our results on the structural parameters were corroborated later in a study of the $RFe_{12-x}Ta_x$ compounds and their hydrides and carbides [5]. The same authors have also studied the $HoFe_{11.4}Ta_{0.6}X_y$ (X ≡ H, C) compounds by means of magnetic measurements and neutron diffraction experiments [6].

0953-8984/00/102265+14$30.00

Table 1. Curie temperatures T_c, easy-magnetization directions EMD at 300 K, spin-reorientation transition temperatures T_s and saturation magnetizations M_s for the $RFe_{11.5}Ta_{0.5}$ compounds from reference [3]. M_n is the total magnetization calculated from the present neutron diffraction measurements.

				M_s (μ_B fu^{-1})		M_n (μ_B fu^{-1})	
Compound	T_c (K) $\pm$ 2 K	EMD at 300 K	T_s (K) $\pm$ 5 K	5 K	300 K	5 K	300 K
$LuFe_{11.5}Ta_{0.5}$	499	$\parallel \boldsymbol{c}$	—	20.9	18.3	23(2)	21(2)
$ErFe_{11.5}Ta_{0.5}$	532	$\parallel \boldsymbol{c}$	40	12.5	15.2	14(2)	17(2)
$HoFe_{11.5}Ta_{0.5}$	541	$\parallel \boldsymbol{c}$	—	12.3	14.5	14(2)	15(2)
$DyFe_{11.5}Ta_{0.5}$	550	$\parallel \boldsymbol{c}$	210, 265	11.7	14.2	13(2)	16(2)
$TbFe_{11.5}Ta_{0.5}$	576	$\perp \boldsymbol{c}$	—	12.4	13.2	14(2)	13(2)

In the present work we perform a systematic study of the crystallographic and magnetic structures of the $RFe_{11.5}Ta_{0.5}$ (R $\equiv$ Tb, Dy, Ho, Er and Lu) series carried out by means of powder neutron diffraction. This work completes the previous magnetic study, determining the individual magnetic moments of the two sublattices, their thermal evolution and the canting angle at the spin-reorientation transition.

2. Experimental details

Samples were prepared by melting the stoichiometric amounts of the constituent elements in a high-frequency induction furnace, using the cold-crucible method. The crystallinity and homogeneity of the samples were assessed from the x-ray diffraction for powdered samples at room temperature. The homogeneity of the samples was also checked by measuring magnetization curves in a Faraday balance (RT–1075 K). In this case the samples, in the form of small crushed ingots, were enclosed in silica-glass sample holders sealed under argon. The ingots were crushed afresh before the neutron diffraction experiments were carried out. They were sieved to a particle size lower than 20 μm to guarantee random orientation of the crystallites.

Neutron diffraction experiments on the compounds based on R $\equiv$ Tb, Ho and Er were carried out at the E6 single-crystal diffractometer (equipped with a position-sensitive detector) of Berlin Neutron Scattering Centre. All data were taken at neutron wavelength $\lambda = 2.4383$ Å in the 2θ range from 19° to 90° with a step size of 0.1°, in the thermal range 1.5–300 K.

The data on the compounds based on R $\equiv$ Dy and Lu were obtained at the D1B two-axis diffractometer of the ILL. Experiments were performed with $\lambda = 1.2845$ Å, in the 2θ range from 10° to 90° (with a step size of 0.2°), in the thermal range 1.5–RT ($\approx$290 K). For the Tb compound, measurements were also made at higher temperatures in this instrument (400 K $< T <$ 600 K), using the same wavelength and step size.

The nuclear and magnetic structures were refined with the Rietveld method using the Fullprof program [7]. Due to the excessive number of free parameters, we have used the following constraints:

(a) The Ta concentration, $x = 0.5$, was kept fixed in the Rietveld refinements of the neutron data, and the Ta atoms were constrained to be at the 8i sites, according to our previous x-ray diffraction analysis at room temperature [8].

(b) The magnetic structure was assumed to be collinear ferrimagnetic with the R atoms coupled antiparallel to the Fe moments, as is usual for the 1:12 compounds, for relatively low x-values [2, 9].

(c) We have used the Fe magnetic form factor supplied by the Fullprof program [7]—that is, the analytical approximation $Ae^{-as^2} + Be^{-bs^2} + Ce^{-cs^2} + D$, where the coefficients A, a, B, b, C, c and D are taken from the *International Tables for Crystallography* [10].

(d) In the fitting process for the diffraction data for short-wavelength neutrons (R ≡ Lu and Dy), we have left the magnetic moments of the Fe and R sublattices free. In this case there is sufficient angular range to cover nuclear-only peaks, which enables us to derive accurately the nuclear contribution and to obtain the magnetic component very reliably. We have found in this case that the sum of the Fe fitted moments for the $DyFe_{11.5}Ta_{0.5}$ compound give the same value as for $LuFe_{11.5}Ta_{0.5}$ (see tables 2 and 3).

Table 2. Refined lattice parameters, magnetization directions, magnetic moments and reliability factors from neutron diffractograms for the compounds based on R ≡ Lu, Ho and Tb at $T = 1.5$ and 300 K. Interatomic distances d, followed by the numbers of nearest neighbours, are also included. 2a is the site occupied by the R atom.

	$LuFe_{11.5}Ta_{0.5}$		$HoFe_{11.5}Ta_{0.5}$		$TbFe_{11.5}Ta_{0.5}$	
	1.5 K	300 K	1.5 K	300 K	1.5 K	300 K
a (Å)	8.4453(4)	8.4525(5)	8.4734(5)	8.4774(7)	8.5035(5)	8.5090(5)
c (Å)	4.7573(3)	4.7656(3)	4.7665(3)	4.7764(4)	4.7706(3)	4.7831(4)
x 8i	0.3577(2)	0.3570(3)	0.3590(4)	0.3592(6)	0.3575(5)	0.3577(5)
x 8j	0.2787(2)	0.2789(3)	0.2746(6)	0.2805(8)	0.2716(6)	0.2758(5)
θ (deg)	0	0	0	0	90	90
m (μ_B) 8i	2.3(1)	2.1(2)	2.3(1)	2.0(1)	2.2(1)	2.0(1)
m (μ_B) 8j	2.0(2)	1.8(2)	1.9(1)	1.7(1)	2.1(1)	1.8(1)
m (μ_B) 8f	1.7(1)	1.6(1)	1.9(1)	1.6(1)	1.7(1)	1.5(1)
m (μ_B) R	—	—	9.5(4)	4.9(3)	9.2(3)	7.0 (2)
R_{nuc} (%)	3.20	3.8	2.9	1.4	3.5	2.9
R_{mag} (%)	5.7	4.0	5.0	4.8	2.4	3.4
R_{wp} (%)	2.9	3.2	5.1	5.2	6.1	5.1
d (Å) 8i–8i (1)	2.402(4)	2.417(4)	2.388(7)	2.396(6)	2.423(6)	2.422(6)
d (Å) 8i–8i (4)	2.923(1)	2.932(1)	2.921(3)	2.924(2)	2.937(2)	2.941(2)
d (Å) 8i–8j (2)	2.642(2)	2.649(2)	2.615(3)	2.659(3)	2.608(3)	2.647(3)
d (Å) 8i–8j (2)	2.642(2)	2.645(2)	2.639(3)	2.665(3)	2.626(3)	2.641(3)
d (Å) 8i–8f (4)	2.588(1)	2.589(1)	2.600(1)	2.602(1)	2.603(1)	2.607(1)
d (Å) 8j–8j (2)	2.644(2)	2.643(2)	2.701(6)	2.631(6)	2.747(6)	2.698(4)
d (Å) 8j–8f (4)	2.435(1)	2.438(1)	2.439(1)	2.446(1)	2.444(1)	2.450(1)
d (Å) 8f–8f (4)	2.378(1)	2.383(1)	2.383(1)	2.388(1)	2.385(1)	2.391(2)
d (Å) 2a–8i (4)	3.021(2)	3.017(2)	3.043(4)	3.044(5)	3.040(4)	3.044(4)
d (Å) 2a–8j (8)	3.025(2)	3.028(2)	3.054(4)	3.027(4)	3.076(4)	3.059(3)
d (Å) 2a–8f (8)	3.214(1)	3.217(1)	3.224(1)	3.225(1)	3.234(1)	3.237(1)

(e) In the fitting process for the compounds based on R ≡ Tb, Ho and Er, the magnetic structure has been refined constraining the sum of the individual iron moments to be equal to the total magnetization found for the $LuFe_{11.5}Ta_{0.5}$ compound,

$$\sum_k \mu_k(RFe_{11.5}Ta_{0.5}) = M_n(LuFe_{11.5}Ta_{0.5}).$$

This approximation is directly done when the measurement temperatures of the two spectra—for the Lu and R = Tb, Ho, Er compounds—coincide, or by interpolation of the Lu data to the intermediate temperature of the R spectrum, when the measurement temperatures are different. M_n is the total magnetization calculated from the present neutron diffraction measurements. The R moment has been left free in the refinements.

Table 3. Refined lattice parameters, magnetization directions, magnetic moments and reliability factors from neutron diffractograms for the R ≡ Er and Dy compounds, at temperatures below and above those of the spin-reorientation transitions. Interatomic distances d, followed by the numbers of nearest neighbours, are also included. 2a is the site occupied by the R atom.

	$ErFe_{11.5}Ta_{0.5}$			$DyFe_{11.5}Ta_{0.5}$		
	1.5 K	30 K	300 K	1.5 K	250 K	300 K
a (Å)	8.4644(5)	8.4630(5)	8.4760(4)	8.4946(8)	8.4980(8)	8.4997(6)
c (Å)	4.7652(3)	4.7647(3)	4.7794(3)	4.7680(5)	4.7784(5)	4.7807(4)
x 8i	0.3564(5)	0.3560(5)	0.3571(4)	0.3566(5)	0.3561(4)	0.3565(3)
x 8j	0.2761(6)	0.2763(7)	0.2784(5)	0.2760(5)	0.2757(5)	0.2758(4)
θ (deg)	30(1)	25(1)	0	90	44(3)	0
m (μ_B) 8i	2.4(1)	2.4(1)	2.0(2)	2.3(1)	2.1(2)	2.0(1)
m (μ_B) 8j	1.8(1)	1.8(1)	1.8(1)	2.1(1)	1.8(2)	2.0(2)
m (μ_B) 8f	1.8(1)	1.8(1)	1.6(1)	1.7 (1)	1.6(1)	1.6(1)
m (μ_B) R	8.9(3)	8.8(3)	3.6(3)	10.2(2)	6.7(2)	5.6(2)
R_{nuc} (%)	3.9	4.0	4.3	5.2	4.5	3.4
R_{mag} (%)	3.7	2.8	3.7	5.6	7.4	3.7
R_{wp} (%)	5.7	5.4	4.3	2.6	2.2	2.6
d (Å) 8i–8i (1)	2.429(2)	2.436(6)	2.422(5)	2.422(6)	2.423(6)	2.433(4)
d (Å) 8i–8i (4)	2.937(4)	2.939(2)	2.940(2)	2.941(2)	2.940(2)	2.943(2)
d (Å) 8i–8j (2)	2.634(3)	2.636(3)	2.652(2)	2.641(3)	2.632(3)	2.639(3)
d (Å) 8i–8j (2)	2.634(3)	2.633(3)	2.651(2)	2.647(3)	2.640(3)	2.639(3)
d (Å) 8i–8f (4)	2.590(1)	2.589(1)	2.597(1)	2.606(2)	2.602(2)	2.598(1)
d (Å) 8j–8j (2)	2.680(6)	2.677(6)	2.656(4)	2.698(4)	2.704(5)	2.690(3)
d (Å) 8j–8f (4)	2.438(1)	2.438(1)	2.445(4)	2.450(1)	2.446(1)	2.445(1)
d (Å) 8f–8f (4)	2.383(1)	2.382(1)	2.389(1)	2.391(1)	2.389(1)	2.387(1)
d (Å) 2a–8i (4)	3.017(4)	3.014(4)	3.027(3)	3.044(4)	3.037(4)	3.028(3)
d (Å) 2a–8j (8)	3.044(4)	3.043(4)	3.039(3)	3.059(3)	3.059(3)	3.053(2)
d (Å) 2a–8f (8)	3.221(1)	3.220(1)	3.226(1)	3.237(1)	3.233(1)	3.230(1)

We have applied this approximation because in these measurements most of the observed peaks had both nuclear and magnetic contributions. Since the Fe magnetic moments are relatively small, they are significantly affected by minor errors in the determination of the nuclear scale factor. Since the sums of the Fe moments of the Lu and Dy compounds are the same, as mentioned in (d), we have felt it appropriate to impose the same condition in the fitting procedure for the R ≡ Er, Ho and Tb compounds in order to obtain more accurate values for the Fe magnetic moments. The consistency of the results justifies this constraint *a posteriori*.

3. Experimental results and discussion

3.1. $LuFe_{11.5}Ta_{0.5}$ (non-magnetic rare earth)

In our previous work on the $LuFe_{11.5}Ta_{0.5}$ compound we reported that it presents uniaxial anisotropy over the thermal range 5–300 K [3], with the easy-magnetization direction being parallel to the crystallographic c-axis. Since the rare earth is non-magnetic, the results on this compound will be useful for obtaining information on the Fe-sublattice properties.

The neutron diffraction patterns were taken at $T = 1.5$, 100, 200 and 300 K. A typical diffractogram is shown in figure 1, together with the fitted profile and calculated differences. A certain amount of α-Fe impurity (10%) and $TaFe_2$ (5%) were found to coexist in the sample.

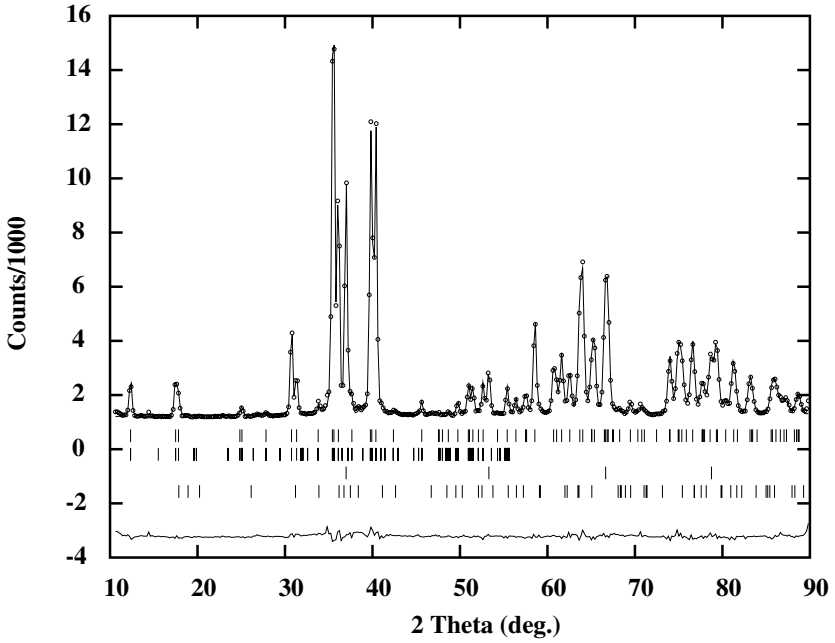

Figure 1. Experimental (dots) and calculated (lines) neutron powder diffraction pattern for the $LuFe_{11.5}Ta_{0.5}$ compound at $T = 1.5$. The difference pattern (observed − calculated) and the calculated peak positions for the main phase, α-Fe and $TaFe_2$ are shown at the bottom of the diagram.

The final fit parameters corresponding to the lowest and highest measurement temperatures (1.5 and 300 K) are included in table 2.

The compound is found to be uniaxial over the thermal range studied, 1.5–300 K, confirming our previous magnetic measurements. The thermal evolutions of the cell parameters and magnetic moments are shown in figures 2 and 3, respectively.

We note that the cell parameters obtained from the neutron diffraction experiments at room temperature are slightly smaller than those previously obtained from the x-ray diffraction analysis [3]. The latter parameters have to be considered as more accurate, because of the uncertainty in the wavelength calibration of the neutron diffractometer.

From table 1 we can observe that the total magnetization $M_n = 23(2)\ \mu_B$ and the average Fe moment $\langle\mu_{\mathrm{Fe}}\rangle_n = 2.0(1)$ obtained from neutron diffraction measurements are slightly larger than the corresponding values $M_s = 20.9\ \mu_B$ and $\langle\mu_{\mathrm{Fe}}\rangle = 1.8\ \mu_B$ deduced from our previous magnetization measurements [3]. We may draw an indirect comparison of M_n with other compounds, taking it into account that the magnetic properties of the $RFe_{12-x}M_x$ series are strongly dependent on the x-value. On one hand it is known that in the $RFe_{11.35}Nb_{0.65}$ series $LuFe_{11.35}Nb_{0.65}$ had a saturation magnetization at 1.5 K practically identical to that of the corresponding Y compound [11]. On the other hand, in the R ≡ Y compounds the saturation magnetization increases linearly for decreasing x, practically irrespective of the M substituted, as was evidenced to happen with M ≡ V, Ti, Cr, W, Nb and Mo [11]. Thus, we may expect a similar relation to hold for the $LuFe_{12-x}M_x$ series. Extrapolating from that phenomenological relation we may expect for $x = 0.5$ the value of 23.5 μ_B fu^{-1}, which corresponds very well with the value 23(1) μ_B fu^{-1} found in our neutron diffraction experiments.

As regards the individual Fe magnetic moments, we note that this is the first neutron

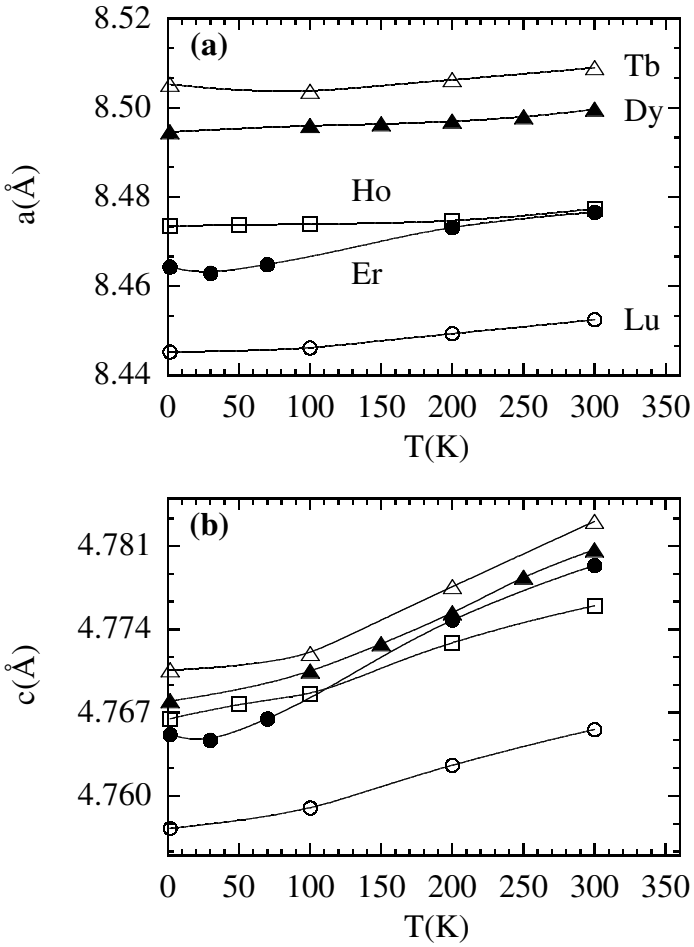

Figure 2. Temperature dependences of the refined lattice parameters a (a) and c (b), for the $RFe_{11.5}Ta_{0.5}$ series.

diffraction determination for a 1:12 compound with non-magnetic R at the minimum M concentration, $x = 0.5$. Consequently, the experimental results obtained at 1.5 K for the Lu compound offer the best opportunity to compare with the calculations [12] or extrapolations [13] performed to evaluate the Fe moments of the hypothetical YFe_{12} phase. The data are compared in table 4. We can see that the μ_{8i}-value deduced for the Lu compound is identical to the theoretical estimation, while the experimental values for μ_{8j} and μ_{8f} are slightly smaller than the calculated ones, though within the range of the experimental error.

Moreover, we have found that the iron magnetic moments follow the trend $\mu_{8i} > \mu_{8j} > \mu_{8f}$, which is obeyed at all measurement temperatures. This hierarchy is observed in other $RFe_{12-x}M_x$ (R non-magnetic) compounds [1, 14, 15], although this is not the only trend found in the literature [1, 16]. However, the observed hierarchy is the most reasonable one in the present case if we consider the following arguments based on the numbers of nearest-neighbouring atoms and distances. In table 2 we have included the number of nearest neighbours for each Fe site z_{ik}, and the interatomic distances d_{ik} between them, derived from the Rietveld refinement (i and k denote the different neighbours). The Fe atom at site 8i has the

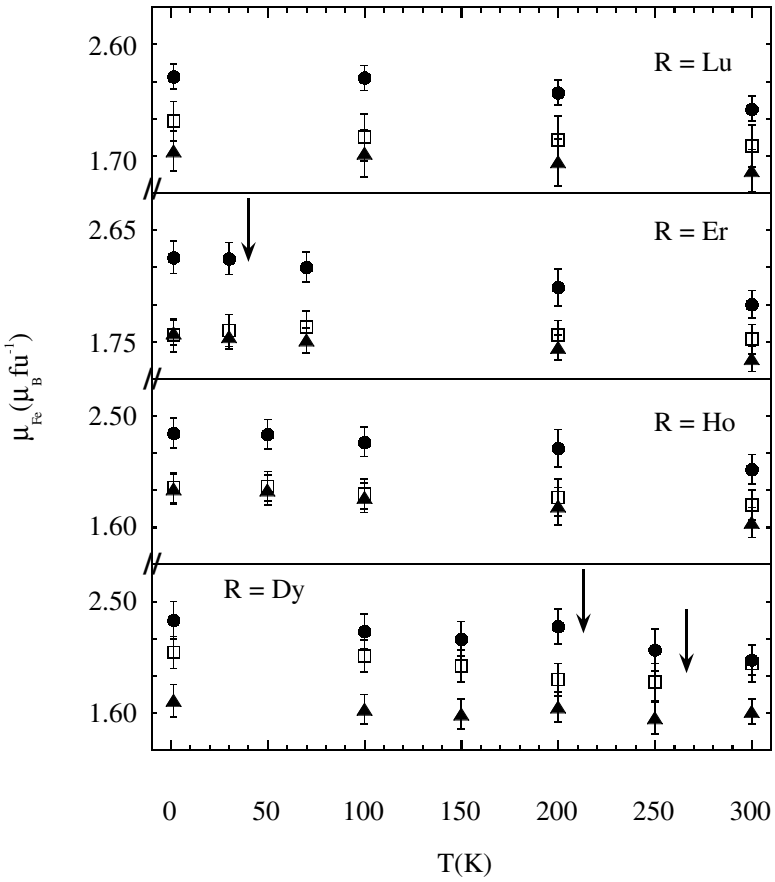

Figure 3. Temperature dependences of the iron magnetic moments 8i (•), 8j (□) and 8f (▲) for the $RFe_{11.5}Ta_{0.5}$, R ≡ Lu, Er, Ho and Dy, compounds. For R ≡ Er and Dy, spin-reorientation transition temperatures are marked by arrows.

Table 4. Comparison of the magnetic moments μ_{8i}, μ_{8j}, μ_{8f} and μ_R among different $RFe_{12-x}M_x$ compounds with relatively low x at different temperatures.

Compound	μ_{8i} (μ_B)	μ_{8j} (μ_B)	μ_{8f} (μ_B)	μ_R (μ_B)	Reference
$LuFe_{11.5}Ta_{0.5}$ (1.5 K)	2.3(1)	2.0(2)	1.7(1)	—	
YFe_{12} (calculated)	2.32	2.26	1.86	—	[12]
YFe_{12} (extrapolated)	2.31	2.17	1.77	—	[13]
$ErFe_{11.5}Ta_{0.5}$ (1.5 K)	2.4(1)	1.8(1)	1.8(1)	8.9(3)	
$ErFe_{10.4}Mo_{1.6}$ (20 K)	1.9(1)	1.8(1)	1.6(1)	9.0(3)	[20]
$ErFe_{11.5}Ta_{0.5}$ (300 K)	2.0(2)	1.8(1)	1.6(1)	3.6(3)	
$ErFe_{11.35}Nb_{0.65}$ (300 K)	2.0(5)	1.9(5)	1.8(3)	3.4(5)	[11]
$HoFe_{11.5}Ta_{0.5}$ (1.5 K)	2.3(1)	1.9(1)	1.9(1)	9.5(4)	
$HoFe_{11}Ti$ (4.2 K)	2.1(2)	2.0(1)	1.9(1)	9.4(3)	[22]
$HoFe_{11.4}Ta_{0.6}$ (4 K)	2.0(2)	2.0(1)	1.8(1)	10.00(2)	[6]

largest number of Fe nearest neighbours, $Z(8i) = 12.4$, while $Z(8j) = Z(8f) = 9.5$ (87.5% of the 8i sites are occupied by Fe atoms). Also, the average interatomic distances, calculated

with the following expressions:

$$\langle d_{\mathrm{Fe-Fe}}\rangle_k = \left(\sum_i z_{ik} d_{ik}\right) \Big/ Z_k \tag{3.1}$$

where

$$Z_k = \sum_i z_{ik} \tag{3.2}$$

are $\langle d_{\mathrm{Fe-Fe}}\rangle_k \approx 2.69$, 2.56 and 2.48 Å for the $k =$ 8i, 8j and 8f sites, respectively.

The local polarization effects associated with the larger coordination number render the 8i site preferential for the localization of the Fe magnetic moment. In spite of the 8j and 8f sites having the same coordination number, a preference towards the 8j site is thought to arise thanks to hybridization effects. Consequently, one expects that the Fe magnetic moments follow the trend $\mu_{8\mathrm{i}} > \mu_{8\mathrm{j}} > \mu_{8\mathrm{f}}$, in accordance with our results. Moreover, this hierarchy is supported by the fact that the same trend is found in the Wigner–Seitz cell volumes of the 3d-metal sites, calculated for R(Fe, M)$_{12}$ compounds [17].

We have used our results on the refined μ_{Fe}-values to obtain information about the nature of the ferromagnetism of the 3d sublattice, using the magnetic valence model [1, 18]. This model is based on the assumption that magnetic moments on the 3d elements of an alloy depend only on composition, via the total number of electrons. Magnetic valence is defined as $Z_m = 2N_{\mathrm{d}} - Z_c$, where N_{d} is the number of electrons of the d band, which is supposed to be five for the 3d elements and zero for rare earths and early transition elements, and Z_c is the chemical valence. The averaged magnetic valence of the $LuFe_{11.5}Ta_{0.5}$ compound is $\langle Z_m\rangle = 2N_{\mathrm{d}} - Z_c = 1.35$. According to this model, which assumes strong ferromagnetism, the average magnetic moment is given by $\langle\mu\rangle = \langle Z_m\rangle + 2N_{\mathrm{sp}}$, where N_{sp} is the number of electrons in the sp band ($\langle\mu\rangle$ and $\langle Z_m\rangle$ are averaged over all the constituents). An alloy is considered a strong ferromagnet if $\langle\mu\rangle$ lies between the values $\langle\mu\rangle = \langle Z_m\rangle + 0.9$ ($N_{\mathrm{sp}} \approx 0.45$) and $\langle\mu\rangle = \langle Z_m\rangle + 0.6$ ($N_{\mathrm{sp}} \approx 0.3$), and a weak ferromagnet below the latter value. The average magnetic moment calculated from our neutron diffraction results for the Fe moments is $\langle\mu\rangle = 1.77\ \mu_B$, which falls below the $\langle\mu\rangle = (\langle Z_m\rangle = 1.35) + 0.6$ line and so indicates that the compound is a weak ferromagnet, like other Fe-rich 1:12 phases such as $YFe_{11}Ti$ [19], $YFe_{11.35}Nb_{0.65}$ [11] and $YFe_{11.5}Mo_{0.5}$ [4].

3.2. $ErFe_{11.5}Ta_{0.5}$

In our previous magnetic measurements on the $ErFe_{11.5}Ta_{0.5}$ compound, axial at $T = 300$ K, we found evidence of a spin-reorientation transition at $T_s = 40$ K, probably to a conical phase [3]. We have performed neutron diffraction experiments below ($T =$ 1.5, 30 K) and above T_s ($T =$ 70, 200 and 300 K).

The final fit parameters of the Rietveld refinements corresponding to $T =$ 1.5, 30 and 300 K are listed in table 3. We have found that small quantities of α-Fe (3%), $TaFe_2$ (6%) and Er_2Fe_{17} (1%) are present in the sample. From the fit of the diffractograms we have obtained a canting angle ranging from 25(1)° at 30 K to 30(1)° at 1.5 K. This result confirms and gives a quantitative value for our previously proposed spin-reorientation transition to a conical phase at $T_s = 40$ K [3]. The thermal evolutions of the cell parameters and the magnetic moments obtained from the Rietveld refinements are depicted in figures 2, 3 and 4.

The Fe-sublattice magnetic moments obey the hierarchy $\mu_{8\mathrm{i}} > \mu_{8\mathrm{j}} \approx \mu_{8\mathrm{f}}$, within experimental error. The values $\langle d_{\mathrm{Fe-Fe}}\rangle \approx$ 2.70, 2.57 and 2.49 Å for the 8i, 8j and 8f iron sites, respectively, were obtained from the distances quoted in table 3. The value of the Er moment, $\mu_{\mathrm{Er}} = 8.9(3)\ \mu_B$ at 1.5 K, is very near to the free-ion value (9 μ_B) and is consistent

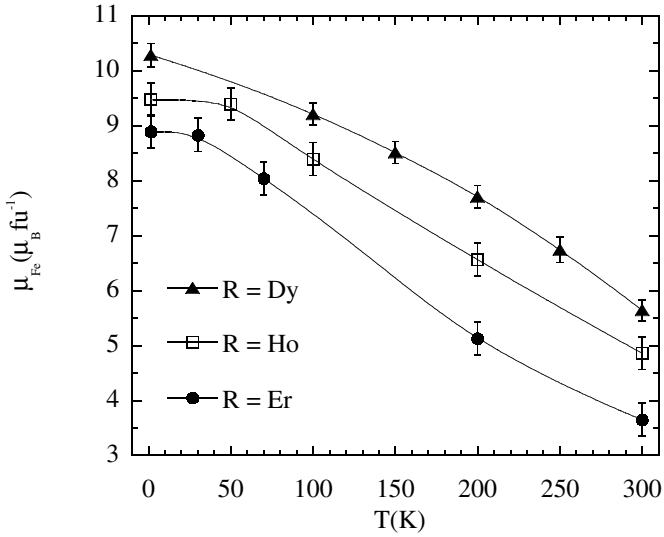

Figure 4. The temperature dependence of the rare-earth magnetic moment for the $RFe_{11.5}Ta_{0.5}$ (R ≡ Er, Ho and Dy) compounds.

with the values derived from neutron diffraction experiments at low temperatures for other Er-based 1:12 compounds [20, 21]. In particular, we have found that the Fe and R magnetic moments measured at 300 K are practically identical to those found for $ErFe_{11.35}Nb_{0.65}$ at the same temperature [11] (see table 4). The total magnetization, as determined from neutron diffraction refinements, M_n, is a few per cent larger than the value M_s found in our previous magnetic measurements (table 1).

3.3. $HoFe_{11.5}Ta_{0.5}$

The Ho compound was found to be uniaxial over the thermal range 5–300 K [3]. We have performed neutron diffraction measurements at $T = 1.5$, 50, 100, 200 and 300 K. The refinement results are summarized in table 2 for $T = 1.5$ and 300 K. Some quantities of α-Fe (4%), $TaFe_2$ (7%) and Ho_2Fe_{17} (4%) have been found in the Rietveld refinements. The neutron diffraction results confirm that the compound is axial over the thermal range 1.5–300 K.

The thermal evolutions of the lattice parameters and the magnetic moments are displayed in figures 2, 3 and 4. The increase of the cell parameters with temperature just reflects the thermal expansion of the compound.

The magnetic moments decrease smoothly with increasing temperature and follow the hierarchy $\mu_{8i} > \mu_{8j} \approx \mu_{8f}$. In this case $\langle d_{Fe-Fe} \rangle \approx 2.70$, 2.57 and 2.49 Å for the 8i, 8j and 8f iron sites, respectively. We observe that the Fe and Ho moments are practically identical to the available values for $HoFe_{11}Ti$ [22] and $HoFe_{11.4}Ta_{0.6}$ [6] (see table 4).

The values for the total magnetization M_n are again a bit higher than M_s. The value for the Ho moment determined by the Rietveld refinement of the neutron diffraction data, $\mu_{Ho} = 9.5(4)\ \mu_B$, is very near to the free-ion value (10 μ_B), and higher than the previous value deduced from the magnetization data, $\mu_{Ho} = 8.4\ \mu_B$.

3.4. $DyFe_{11.5}Ta_{0.5}$

In our previous magnetic study on $DyFe_{11.5}Ta_{0.5}$, we reported that this compound has two spin-reorientation transitions, one from axial to conical at $T_{s1} = 265$ K and a second one at $T_{s2} = 185$ K, that we proposed would prove to be a transition from conical to basal

anisotropy [3].

To check these results and conjectures we have performed neutron diffraction measurements at $T = 1.5$, 100, 150, 200, 250 and 300 K. The final fit parameters of the Rietveld refinements corresponding to $T = 1.5$, 250 and 300 K are listed in table 3. No constraints have been imposed on the Fe magnetic moments in this case. We have found certain quantities of α-Fe (4%) and $TaFe_2$ (7%) in the refinement procedure.

At room temperature ($\approx$290 K) we have found that the anisotropy is uniaxial; i.e. $\theta = 0^\circ$. At $T = 250$ K, below T_{s1}, the compound is in a conical phase with a canting angle of $\theta = 44(3)^\circ$, in agreement with the previously proposed spin-reorientation transition from an axial to a conical phase at $T_{s1} = 265$ K. However, at $T = 200$ K, also in the region between the two initially proposed spin-reorientation transitions, we obtain from the fit that $\theta = 90^\circ$—that is, the compound is already in the planar phase.

This result is apparently in contradiction with our previous determination of $T_{s2} = 185$ K, which was deduced from a change in slope in the $M_\perp(T)$ measurements [3]. It is now evident from the above paragraph that $T_{s2} > 200$ K. In our magnetization measurements we noticed a small change of slope at 210 K, that we now tentatively propose as the revised T_{s2}. Though this spin-reorientation transition is expected to be of first order by analogy with other $DyFe_{12-x}M_x$ compounds, the magnetization may not change abruptly below T_{s2}. The reason for this is that in such a first-order transition there may be a coexistence of the conical and basal phases. The volume ratio of one phase with respect to the other varies progressively as temperature is lowered, as has been proven to occur in the $DyFe_{11}Ti$ compound [23]. As a consequence, the $M_\perp(T)$ curve varies continuously from the onset T_{s2} until the whole system has transformed to basal. In our view, in $DyFe_{11.5}Ta_{0.5}$ the spin-reorientation transition starts at the first change of slope, $T_{s2} = 210$ K, and the total transformation ends at 185 K, causing the second change of slope. Thus, at 200 K our neutron diffraction data show that the majority phase is basal.

Thermal variations of the cell parameters and magnetic moments are displayed in figures 2, 3 and 4. The increase in the cell parameters does not reflect any significant change at the transition temperatures. The average distances are $\langle d_{Fe-Fe} \rangle \approx 2.70$, 2.57 and 2.50 Å for the 8i, 8j and 8f sites respectively. No departure from the smoothly interpolated expected values was found to occur in the interatomic distances at the spin-reorientation transitions. In contrast, we find some evidence of changes in the magnetic moments near the temperatures at which the spin-reorientation transitions take place. At $T = 200$ K we have found a net increase in μ_{8i} and μ_{8f}, while at room temperature ($\approx$290 K) an anomalous increase in μ_{8j} is observed.

As for $LuFe_{11.5}Ta_{0.5}$, the hierarchy $\mu_{8i} > \mu_{8j} > \mu_{8f}$ is obeyed at all temperatures and the values of the Fe moments at the different sites, as well as the total iron magnetization, are in very good agreement for the two compounds (tables 2 and 3). This is especially relevant since there were no constraints imposed in the fitting process for either sample. This result supports, as explained in section 2, the constraint of a constant sum of Fe moments in the analysis of the compounds based on Er, Ho and Tb. The Dy moment $\mu_{Dy} = 10.3(2)\ \mu_B$, found at $T = 1.5$ K, is very near the free-ion value ($10\ \mu_B$) and quite a bit larger than the value $9\ \mu_B$ deduced from magnetization measurements, probably because of the accumulated errors in the latter.

3.5. $TbFe_{11.5}Ta_{0.5}$

In our previous magnetic study on the Tb compound we found that it remains planar over the thermal range 5–300 K [3]. We have performed neutron diffraction measurements at $T = 1.5$, 100, 200 and 300 K with a wavelength of $\lambda = 2.4383$ Å. The refinement results are summarized in table 2 for $T = 1.5$ and 300 K. Small quantities of α-Fe (3%), $TaFe_2$ (4%) and Tb_2Fe_{17} (2%) were found to coexist in the sample. The thermal evolution of the lattice parameters is

displayed in figure 2.

The refinement results displayed in table 2 and figure 5 show that this compound has planar anisotropy between 1.5 and 300 K and that the Fe magnetic moments obey the trend $\mu_{8i} > \mu_{8j} > \mu_{8f}$. Again, this trend is supported by the trend of the average distances $\langle d_{Fe-Fe} \rangle \approx 2.70$, 2.57 and 2.50 Å for 8i, 8j and 8f sites, respectively. The Tb moment at 1.5 K is $\mu_{Tb} = 9.2(3)\ \mu_B$, very near the free-ion value (9 μ_B) and, again, somewhat larger than the value deduced from magnetization measurements (8.5 μ_B).

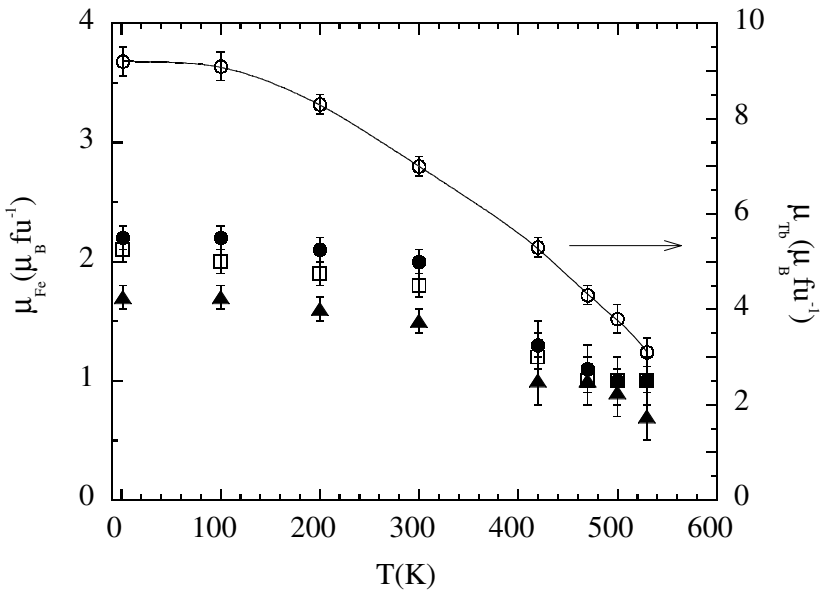

Figure 5. Temperature dependences of the rare-earth (○) and iron magnetic moments 8i (●), 8j (□) and 8f (▲) for the $TbFe_{11.5}Ta_{0.5}$ compound.

Notwithstanding these results, we wished to verify that there is no spin-reorientation transition from axial to basal at temperatures higher than room temperature. This kind of transition has been detected for other $TbFe_{12-x}M_x$ compounds, such as $TbFe_{11}Ti$, with $T_s = 330$ K [24], and $TbFe_{10.5}Mo_{1.5}$, with $T_s = 190$ K [25]. To explore that possibility we performed neutron diffraction experiments at $T = 400$, 470, 500, 530 and 600 K. In this case we used a wavelength of $\lambda = 1.2845$ Å and no constraints were imposed on the Fe magnetic moments. Magnetic moments are displayed in figure 5. We have found that the compound is clearly planar up to 400 K. For higher temperatures, the present neutron diffraction data are not very sensitive to small changes in the magnetization direction because the magnetic moments are relatively small. However, we did not detect any abrupt change in angle, and the fits are in reasonable agreement ($R_{nuc} = 4.1$, $R_{mag} = 7.6$ and $R_{wp} = 3.1$ at $T = 500$ K) with basal anisotropy. Thus we conclude that, within our experimental resolution, no spin reorientation is present in this compound over the 1.5–T_c thermal range, which is consistent with the results obtained by Hu *et al* for the $TbFe_{11.35}Nb_{0.65}$ compound [11].

4. Conclusions

The magnetic structures of $RFe_{11.5}Ta_{0.5}$ (R ≡ Tb, Dy, Ho, Er and Lu) have been determined for the thermal range 1.5–300 K by means of neutron powder diffraction experiments, confirming

our previous results derived from magnetization measurements [3]. We have verified that no spin-reorientation transitions are present in the Ho and Lu compounds; the magnetic anisotropy remains uniaxial over the cited thermal range. The canted low-temperature phase ($T < T_s = 40$ K) of the Er compound has been confirmed; we find a maximum canting angle of 30° at 1.5 K. In the Dy compound the two spin-reorientation transitions have also been confirmed: from axial to conical at $T_{s1} = 265$ K and from conical to planar at $T_{s2} \approx 210$ K. We have revised the value of T_{s2} obtained in our previous magnetic study. For the R ≡ Tb compound we have determined that, within our experimental resolution, the compound remains planar over the thermal range 1.5 K–T_c.

From the Rietveld analysis of the neutron diffraction measurements, the total magnetization M_n, calculated as the algebraic sum of the Fe and R moments, is in all measurement cases about 10% larger than the corresponding value derived from magnetization measurements at the same temperature. We think that this discrepancy is caused by some misalignment of the grains in the oriented powder used in the magnetization measurements, which reduces the projection of the moments along the easy-magnetization direction.

The refined μ_R-values at $T = 1.5$ K are very near to their free-ion value. In general, they are higher than the values deduced from our previous magnetic measurements, probably due to the accumulated errors in those determinations.

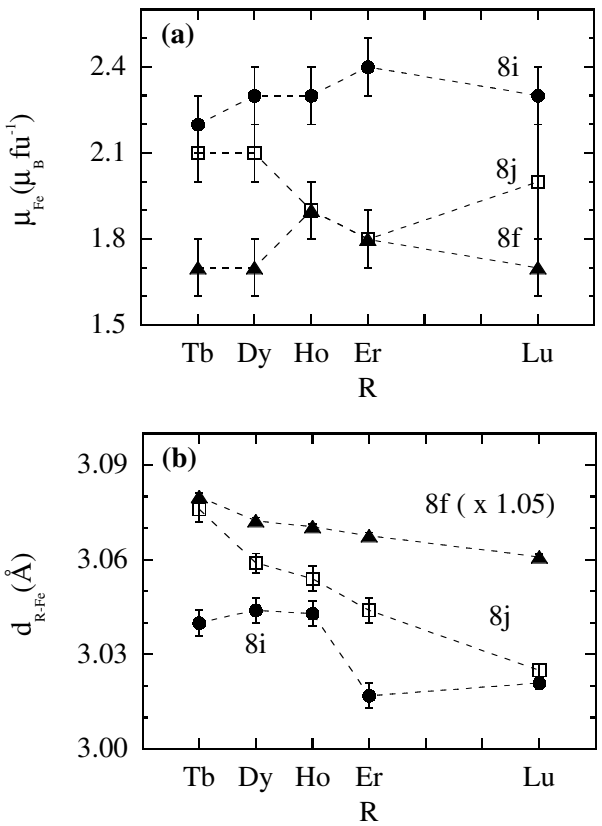

Figure 6. Evolution of the individual Fe magnetic moments μ_k (a) and the R–Fe distances d_{R-k} (b), across the lanthanide series. k stands for the different crystallographic sites for the Fe atoms: 8i (•), 8j (□) and 8f (▲).

We have found that the different Fe magnetic moments follow the trend $\mu_{8i} > \mu_{8j} \geqslant \mu_{8f}$ for all compounds. The observed hierarchy in the Fe magnetic moments is consistent with the Fe coordination number, $Z(8i) = 12.4 > Z(8j) = Z(8f) = 9.4$, with the hierarchy in the Wigner–Seitz volumes, $V(8i) > V(8j) > V(8f)$ [17], and with the average Fe–Fe distances, $\langle d_{Fe-Fe}\rangle_{8i} \approx 2.70$ Å $> \langle d_{Fe-Fe}\rangle_{8j} \approx 2.57$ Å $> \langle d_{Fe-Fe}\rangle_{8f} \approx 2.50$ Å. That is, the local polarization effects of the Fe sublattice and the degree of orbital overlap with the surrounding atoms seem to have a direct influence on the strength of the Fe local magnetic moments.

In figure 6(a) we have depicted the variation of the Fe individual magnetic moments at 1.5 K across the lanthanide series. Although the experimental errors in the determination of the Fe magnetic moments are large, a trend is clearly observed: for magnetic R the μ_{8j}-moment decreases with respect to the μ_{8i}-value, approaching the value of μ_{8f}. This trend in the Fe moments cannot be related to the $\langle d_{Fe-Fe}\rangle$ distances, which do not change appreciably across the lanthanide series. However, it may be correlated with the influence of the R atom. The 8i Fe atom has one R atom as a nearest neighbour at ≈3.03 Å, while the 8j and 8f atoms each have two R atoms at ≈3.05 and 3.22 Å, respectively. Also, although the hierarchy $d_{R-8f} > d_{R-8j} > d_{R-8i}$ is maintained across the lanthanide series, the distance d_{R-8j} decreases more strongly than the distances d_{R-8i} and d_{R-8f} (figure 6(b)). Consequently, the Fe moment at the 8j site is the most sensitive to the R influence, and the progressive decrease across the lanthanide series may be explained as due to the hybridization with the rare-earth atom.

Acknowledgments

This work was financed by the MAT96/448 CICYT project (Spanish Government) and partly by the EC project MAGNET BRR-CT-97-5014. C Piquer thanks CICYT for her Doctoral grant PN973195091. The Collaborating Research Group (CRG) D1B, supported by CSIC/CICYT (Spain) and the CNRS (France), is acknowledged for the allocation of beam time at the D1B instrument.

References

[1] Li H and Coey J M D 1992 *Handbook of Magnetic Materials* vol 6, ed K H J Buschow (Amsterdam: North-Holland) p 1 and references therein
[2] Buschow K H J 1991 *Rep. Prog. Phys.* **549** 1123
[3] Piquer C, Artigas M, Rubín J and Bartolomé J 1998 *J. Phys.: Condens. Matter* **10** 11 055
[4] Sun H, Akayama M, Tatami K and Fujii H 1993 *Physica* B **183** 33
[5] Vert R, Boudina M, Fruchart D, Gignoux D, Kalychak Y M and Skolozdra R V 1999 *J. Alloys Compounds* **287** 38
[6] Vert R, Boudina M, Fruchart D, Gignoux D, Kalychak Y M, Ouladdiaf B and Skolozdra R V 1999 *J. Alloys Compounds* **285** 56
[7] Rodríguez-Carvajal J 1990 *Proc. Satellite Mtg on Powder Diffraction; 15th Congr. of the IUCr (Toulouse)* p 127
[8] Artigas M, Piquer C, Rubín J and Bartolomé J 1999 *J. Magn. Magn. Mater.* **196+197** 653
[9] Al-Omari I A, Jaswall S S, Fernando A S, Sellmyer D J and Hamdeh H H 1994 *Phys. Rev.* B **50** 12 665
[10] *International Tables for Crystallography* 1992 vol C, ed A C J Wilson (Dordrecht: Kluwer) p 391
[11] Hu Bo-Ping, Wang Kai-Ying, Wang Yi-Zhong, Wang Zhen-Xi, Yang Qi-Wei, Zhang Pan-Lin and Sun Xiang-Dong 1995 *Phys. Rev.* B **51** 2905
[12] Coehoorn R 1990 *Phys. Rev.* B **41** 11 790
[13] Denissen C J M, Coehoorn R and Buschow K H J 1990 *J. Magn. Magn. Mater.* **87** 51
[14] Ayres de Campos J, Ferreira L P, Godinho M, Gil J M, Mendes P J, Ayres de Campos N, Ferreira I C, Boudina M, Bacmann M, Soubeyroux J L, Fruchart D and Collomb A 1998 *J. Phys.: Condens. Matter* **10** 4101
[15] Mao W, Yang J, Cui B, Cheng B, Yang Y, Du H, Zhang B, Ye C and Yang J 1998 *J. Phys.: Condens. Matter* **10** 2611
[16] Sun H, Morii Y, Fujii H, Akayama M and Funahashi 1993 *Phys. Rev.* B **48** 13 333

[17] Isnard O and Fruchart D 1994 *J. Alloys Compounds* **205** 1
[18] Williams A R, Moruzzi V L, Malozemoff A P and Terakura K 1983 *IEEE Trans. Magn.* **19** 1983
[19] Hu B, Li H, Gavigan J P and Coey J M D 1989 *J. Phys.: Condens. Matter* **1** 755
[20] Rubín J, Garitaonandia J S, Bartolomé J, Barandiaran M, Palacios E, Fruchart D and Miraglia S 1998 *Solid State Commun.* **106** 821
[21] Tomey E P 1994 *Thesis* Université Joseph Fourier, Grenoble
[22] Obbade S, Fruchart D, Boudina M, Miraglia S, Soubeyroux J L and Isnard O 1997 *J. Alloys Compounds* **253+254** 298
[23] Algarabel P A, Ibarra M R, Bartolomé J, García L M and Kuz'min M D 1994 *J. Phys.: Condens. Matter* **6** 10 551
[24] Abadía C, Algarabel P A, García-Landa B, Ibarra M R, del Moral A, Kudrevatykh N V and Markin P E 1998 *J. Phys.: Condens. Matter* **10** 349
[25] Tomey E, Bacmann M, Fruchart D, Soubeyroux J L and Gignoux D 1995 *J. Alloys Compounds* **231** 195